Chinese Chemical Letters 34 (2023) 107820

Contents lists available at ScienceDirect

Chinese Chemical Letters

journal homepage: www.elsevier.com/locate/cclet

Modification and application of Fe_3O_4 nanozymes in analytical chemistry: A review

Jiahe Ju[a], Yitong Chen[a], Zhiqiang Liu[a], Cheng Huang[a], Yaqi Li[b], Dezhao Kong[b,*], Wei Shen[a], Sheng Tang[a,*]

[a] School of Environmental and Chemical Engineering, Jiangsu University of Science and Technology, Zhenjiang 212003, China
[b] School of Grain Science and Technology, Jiangsu University of Science and Technology, Zhenjiang 212003, China

ARTICLE INFO

Article history:
Received 9 June 2022
Revised 21 August 2022
Accepted 12 September 2022
Available online 15 September 2022

Keywords:
Fe_3O_4 nanomaterials
Nanozyme
Peroxidase-like activity
Modification
Application

ABSTRACT

In recent years, Fe_3O_4 nanomaterials have received much attention in analytical chemistry due to their excellent magnetic and peroxidase-like activity. As the catalytic characteristics of Fe_3O_4 nanomaterials is similar to those of horseradish peroxidase (HRP), Fe_3O_4 nanomaterials are also used as peroxidase mimics and have achieved a certain development in many fields based on latest research results. To improve the stability and catalytic ability of simple Fe_3O_4 nanomaterials, various modification strategies of Fe_3O_4 nanomaterials have been developed. The recent advances of these strategies have been presented and discussed. In addition, this paper introduces the application of Fe_3O_4 nanozymes in the detection of food and industrial pollutants, as well as in the field of biosafety.

1. Introduction

With excellent magnetic properties, Fe_3O_4 nanomaterials can assemble rapidly under the action of an external magnetic field and then redisperse in solution without the external magnetic field [1,2]. In addition, based on their good biocompatibility, Fe_3O_4 nanomaterials can also be widely used in biomedicine for magnetic resonance imaging [3] or object separation and purification [4]. Since 2007, ferromagnetic nanoparticles (NPs) have been found to have intrinsic peroxidase-like activity [5], which is similar to natural horseradish peroxidase (HRP), a protein containing heme and can oxidize different peroxidase substrates and produce color changes in the presence of hydrogen peroxide (H_2O_2). For example, 3,3′,5,5′-tetramethylbenzidine (TMB), di-azo-aminobenzene (DAB), *o*-phenylenediamine (OPD) and 2,2′-azino-bis(3-ethylbenzothiazoline-6-sulfonic acid) diammonium salt (ABTS) can be catalyzed by Fe_3O_4 nanomaterials to be blue, brown, orange and green in the presence of H_2O_2, respectively. Based on this discovery, the term "artificial nanozyme" was introduced to classify nanomaterials with enzyme-like activity. Compared to natural enzymes, the peroxidase-like activity of Fe_3O_4 nanozymes can overcome a series of shortages, such as inactivation under high temperature or extreme pH, high preparation cost, difficult storage With the advantages of simple preparation, large output and adjustable catalytic activity, Fe_3O_4 nanozymes can replace the natural enzyme in different aspect [6]. However, the Fe_3O_4 nanozyme is aggregated easily in water due to its instability and poor dispersibility [7]. So, the modification of Fe_3O_4 nanozymes to maintain their characteristics has become a focus of research.

The modification methods and peroxidase-like activity of Fe_3O_4 nanozymes has been reported in many manuscripts and has been gradually applied in different fields nowadays. Among iron-based nanomaterials, Fe_2O_3 also can be applied as a nanozyme. However, it is difficult to synthesize the Fe_2O_3 nanoparticles with uniform and adjustable size, and the obtained Fe_2O_3 nanozyme is also easy to aggregate. Compared with Fe_2O_3 nanozyme, Fe_3O_4 nanozyme has a simpler synthesis method and higher activity since the concurrence of Fe^{2+} and Fe^{3+} could accelerate the catalytic process [8]. In reaction process, the Fe^{3+} was partially reduced to Fe^{2+}, which activated H_2O_2 to generate ·OH firstly, and then Fe^{2+} was oxidized to Fe^{3+} by H_2O_2. Therefore, Fe_3O_4 nanozyme are more widely used, which was focused by this review. Except of ferromagnetic nanomaterials, carbon-based nanomaterials [9], vanadium-based nanomaterials [10], noble metal materials [11–13], *etc.* also have peroxidase-like activity. However, Fe_3O_4 nanozymes, as a perioxidase mimic, were widely used in different areas due

* Corresponding authors.
E-mail addresses: kdz1011@just.edu.cn (D. Kong), tangsheng.nju@gmail.com (S. Tang).

https://doi.org/10.1016/j.cclet.2022.107820
1001-8417/

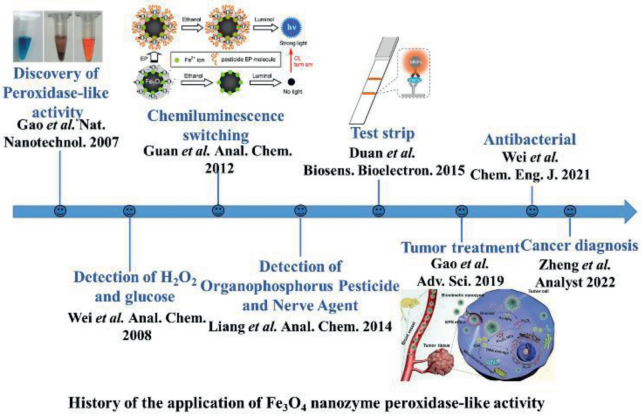

Fig. 1. A brief timeline for the development of Fe_3O_4 nanozyme. Reprinted with permission [5]. Copyright 2007, Springer Nature. Reprinted with permission [18]. Copyright 2012, American Chemical Society. Reprinted with permission [21]. Copyright 2015, Elsevier. Reprinted with permission [24]. Copyright 2018, Wiley-VCH Verlag.

to the excellent magnetic properties. For example, the Fe_3O_4 can be isolated by magnet easily after capturing targets, resulting in a quick target enrichment. In some studies, a 2D or 3D Fe_3O_4 network can be formed and presented an enhanced peroxidase-like activity [14,15]. Such advantages are not available in other materials.

Ever since the founding of peroxidase-like activity of ferromagnetic NPs, it has been used for analyte detection. The brief development process of the Fe_3O_4 nanozyme is shown in Fig. 1. Several representative applications of Fe_3O_4 nanozymes were listed from 2007 to 2022. In 2008, Wang *et al.* used Fe_3O_4 magnetic NPs (MNPs) for H_2O_2 detection based on the simple application of catalytic properties [16]. Subsequently, further research was conducted to modify the Fe_3O_4 nanozyme for wider application. In biosafety detection, Fe_3O_4 nanozymes can be used to detect cancer markers, such as carcinoembryonic antigen and α-fetoprotein [17]. In addition, the highly sensitive detection of pesticides and nerve agents also provides a faster and convenient way for food safety detection [18–20]. After that, MNP was used as a nanozyme probe to develop an immunochromatographic strip for Ebola virus detection in 2015 [21]. In the biomedical field, Fe_3O_4 nanozyme with peroxidase-like activity can produce ·OH in the presence of H_2O_2 to achieve bactericidal and anti-inflammation effects [22,23]. Therefore, cancer treatment applications have been developed based on this property [24–26].

To date, some reviews on nanozymes have been published, but the scope of these reviews is very broad. Some reviews summarize various nanozymes with enzymatic activities, such as peroxidase, oxidase, catalase, and superoxide dismutase [27–30]. Some reviews only focused on the physical property of magnetic iron oxide nanostructures synthesized by different methods [31]. Some reviews emphatically introduced the specific application of nanozymes, such as energy and industrial sectors [31], food safety analysis [32,33], environmental analysis [34], and biomedical field [35–37]. In our manuscript, we detailed introduced the different synthesis methods of Fe_3O_4 nanozymes and discussed the influence on size and morphology of synthesized nanozymes. Various modification strategies for Fe_3O_4 nanozymes and the resulted catalytic performance were emphatically reviewed. Also, the catalytic mechanism and affect factors were discussed. In addition, the application of Fe_3O_4 nanozyme has been comprehensively studied, including food safety, industrial pollution and biosafety. Finally, this article also proposed some possible challenges and expectations in the application of Fe_3O_4 nanozymes.

Table 1
Several typical methods for the synthesis of Fe_3O_4 nanomaterials.

Method	Structure	Size (nm)	Ref.
Chemical co-precipitation	Sphere	15–30	[38,39]
Solvothermal method	Diverse morphology: spheres, octahedra and triangular plates	200–500	[40-42,44]
Thermal decomposition	Cubic, sphere	< 10	[43,45,46]
Solution gel	Cubic	7.2	[47]
Microwave-assisted solvothermal method	Nanocrystal, nanocluster	12–25 40–90	[48]

2. Synthetic methods

2.1. Synthesis of Fe_3O_4 nanozymes

Fe_3O_4 nanomaterials can be synthesized by different typical methods, such as the chemical co-precipitation method [38,39], solvothermal method [40–42] and thermal decomposition methods [43]. The size and appearance of nanozymes synthesized by different methods are shown in Table 1. It can be seen that the size and morphology of the materials prepared by different synthesis methods are varied. Therefore, it is very important to select the appropriate synthesis method to obtain Fe_3O_4 nanozyme with suitable size and morphology.

2.1.1. Chemical co-precipitation method

For chemical co-precipitation method, the Fe^{3+} and Fe^{2+} with a certain ratio were dissolved in aqueous solution. Meanwhile, the temperature and pH were strictly controlled. In this method, MNPs with small size can be synthesized. The reaction can be expressed as: $2Fe^{3+} + Fe^{2+} + 8OH^- = Fe_3O_4\downarrow + 4H_2O$. Generally, $FeCl_3{\cdot}6H_2O$ and $FeCl_2{\cdot}4H_2O$ were dissolved in distilled water in a molar ratio of 2:1 and protected by nitrogen during the process. The pH value was adjusted to 8.0 by ammonium hydroxide solution. The obtained material is spherical with a size of approximately 15–30 nm. This simple process requires low calcination temperature and short time, and Fe^{3+} and Fe^{2+} can be mixed and precipitated more uniformly.

2.1.2. Solvothermal method

The solvothermal method, first reported in 2005, takes advantage of a simple synthesis process to produce a product with diverse morphology, and better regularity. In this method, the soluble Fe^{3+} salt was reduced and precipitated in ethylene glycol [44]. The obtained monodisperse Fe_3O_4 microspheres with a size at 200–500 nm, and different morphologies can be formed based on different mineralizer types. Shi *et al.* added $FeCl_3{\cdot}6H_2O$ and sodium acetate into ethylene glycol with vigorous stirring, and then reacted in Teflon lined stainless steel autoclaves. The obtained Fe_3O_4 microspheres were isolated by magnetic separation for subsequent treatment [41]. In this method, the change of solvents, mineralizers, and surfactants all will affect the morphology and particle size of the material.

2.1.3. Thermal decomposition method

In this method, the iron precursor generated iron atoms through high-temperature decomposition process, and then generated iron-based NPs. First, $Fe(C_5H_7O_2)_3$ and 1,2-hexanediol were dissolved in benzyl ether and stirred magnetically under the protection of N_2. Then, oleylamine and oleic acid were added, stirred

vigorously again, and heated [45]. The size of obtained Fe_3O_4 nanomaterials can be controlled within 10 nm, and the cubic Fe_3O_4 nanomaterials can be synthesized [46].

2.1.4. Other methods

In addition to the abovementioned methods, some other methods also can be used for Fe_3O_4 nanomaterial synthesis. Song *et al.* used the solution gel method to prepare Fe_3O_4 NPs. A magnetic hydrogel was used as the precursor and synthesized cubic Fe_3O_4 NPs with a diameter of approximately 7.2 nm [47]. Through microwave-assisted solvothermal method, the shortcomings of high temperature and long reaction time can be improved [48]. Monodisperse Fe_3O_4 nanocrystals could be synthesized within 3 h, and the product size could be adjusted.

2.2. Modification

In order to surmount the disadvantages, researchers have focused more attention on the Fe_3O_4 nanozymes modification. By modifying Fe_3O_4 nanozymes with different materials or methods, the stability can be improved and avoid agglomeration in solution. Additionally, catalytic activity also can be improved. This review divides the modifying materials into metals and nonmetals.

2.2.1. Metal material modification

Due to its low price and ease of obtaining, copper (Cu) was widely used in the production of compound nanomaterials [49]. Chen *et al.* synthesized Cu-doped Fe_3O_4 MNPs by ion heating, which can enhance the catalytic activity of nanomaterials base on the similar ion radii of Cu^{2+} and Fe^{2+} [50]. In this method, Fe^{2+} was partially replaced with Cu^{2+}, and Fe^{3+} was reduced by Cu^{2+} ions. The Cu^{2+} ions can also be enriched on the surface through $HOO\cdot$ and promote the regeneration of Fe^{2+}. Therefore, this redox cycle enhanced both the decomposition of H_2O_2 and the peroxidase-like activity of the obtained material. Copper can also be coated on Fe_3O_4 as a peroxidase mimic. Li *et al.* synthesized Fe_3O_4-Cu^{2+} nanocomposites (NCs) by coating Cu on Fe_3O_4 in a two-step method [51]. First, sodium lignin sulfonate (SL) is used to form Fe_3O_4-SL intermediates through alcohol thermal method, and then Cu^{2+} solution is added to produce Fe_3O_4-Cu^{2+} NPs. The synthesized material has excellent catalytic activity, magnetism, and good affinity for color-developing substrates, and can be used as a peroxidase mimic enzyme for colorimetric detection of H_2O_2 by catalytic oxidation of TMB with a detection limit as 0.2 μmol/L.

Recently, some noble metals, such as Au [52], Pt [53] and Pd [54], have attracted more attention due to their special catalytic properties. Jiang *et al.* fixed Pt between core-shell structures and synthesized Fe_3O_4@resorcin/formaldehyde resin-Pt@polydopamine (Fe_3O_4@RF-Pt@PDA) as microspheres material, and took it for colorimetric detection of H_2O_2 and glucose as a mimetic enzyme [55]. The formation of this double-shell structure not only provides active centers for the noble metals which sandwiched between them but also prevents agglomeration of magnetic materials and leaching of noble metals. Therefore, this material has better peroxidase-like activity than HRP. Yang and Wang *et al.* used Pd to enhance the peroxidase-like activity of Fe_3O_4 and synthesized Pd/Fe_3O_4-polyetheylenimine-reduced graphene oxide (Pd/Fe_3O_4-PEI-rGO) nanohybrid materials [56]. Due to the large specific surface area, rGO can prevent Fe_3O_4 from agglomerating in solution and can improve the stability and catalytic activity. In this way, ordinary Fe_3O_4 nanomaterials can take better properties when modified with noble metal material. Except of this monometallic modification of Fe_3O_4 nanomaterials, Zhang *et al.* deposited Au, Pd and Fe_3O_4 on the surface of graphene and synthesized an Au-Pd-Fe_3O_4/rGO complex. This material with three type metals has better peroxidase-like activity, and became a highly efficient and recyclable liquid phase reaction catalyst [57].

The high oxygen storage capacity and simple conversion ability between Ce(III) and Ce(IV) allow CeO_2 NPs to possess peroxidase-like activity. However, different from the back and forth process between Fe^{3+} and Fe^{2+} of Fe_3O_4, Ce^{3+} was oxidized into Ce^{4+} and releasing $\cdot OH$ to oxidize the substrate TMB turn colorless solution become blue. But the Ce^{4+} needs consumption $HO_2\cdot$ species to back to Ce^{3+}. This dynamic equilibrium of Ce^{3+} and Ce^{4+} turns out to slow down the oxidation of substrate. Therefore, Yu prepared Fe_3O_4@CeO_2 eggshell NCs by growing CeO_2 on Fe_3O_4 hollow NPs, this material with intrinsic synergistic effect can be successfully applied for H_2O_2 and glucose detection [58]. Manganese dioxide (MnO_2) also can be used to improve the catalytic capacity of Fe_3O_4 nanozyme. MnO_2 also has peroxidase-like activity with the smaller K_m than Fe_3O_4, which mean it has better catalytic activity. The MnO_2 microspheres doped Fe_3O_4 prepared by a two-step hydrothermal method can form dislocation structures and enhance catalytic activity [59]. This is mainly based on the permeation of iron to the crystal structure of MnO_2, which makes MnO_2 rich in defects, dislocations and vacancies, and increases the number of active centers to produce $\cdot OH$ radicals. Besides, CoO_x, Cu_2O, TiO_2, ZnO, *etc.*, also possess peroxidase-like activity, even better than Fe_3O_4. However, these metal oxides NPs may be limited with aqueous dispersion, separation and recovery in the practical application. Fe_3O_4 NPs can take a synergy with these materials and enhance the catalytic activity. More importantly, the excellent magnetic property of Fe_3O_4 NPs can achieve convenient enrichment and separation or recovery by a magnet.

2.2.2. Nonmetallic material modification

In addition to metal modification of Fe_3O_4 nanomaterials, nonmetal modification is also a common method.

As a type of inorganic nonmetallic material, carbon-based nanomaterials can be widely used to improve the stability of magnetic NCs [60,61]. Carbon quantum dots (C-dots) with intrinsic peroxidase-like activity are effective for Fe_3O_4 nanomaterials modification. The catalytic activity of C-dots/Fe_3O_4 was superior to that of the two separate precursor materials. Wang *et al.* synthesized Fe_3O_4@C NPs with an egg yolk-shell structure for the detection of H_2O_2 and glucose [62]. These Fe_3O_4@C yolk-shell nanostructures (YSNSs) are superior to other intermediate nanomaterials in catalytic activity due to their unique yolk-shell nanostructure. Wang's paper explained that the main reason for the improvement of Fe_3O_4@C YSNS is that the hollow space of the structure can provide a better catalytic microenvironment. The mesoporous channel facilitates the mass transfer and free movement of Fe_3O_4 nuclear energy and can provide more active centers. Moreover, loading magnetic nanomaterials onto nanostructures with large specific surface areas also can reduce the self-aggregation. Carbon nanotubes (CNTs) are one of the nanostructures which can be used to promote the dispersion of Fe_3O_4 NPs and reduce agglomeration. Multiwalled CNTs (MCNTs) can be applied to synthesize Fe_3O_4/MCNT due to the excellent *in-situ* reduction properties. The materials have high peroxidase-like activity over a wide pH range and more stable for hazard removal. Xu and Liu *et al.* reported that naringin can be used as a carbon precursor to synthesize multifunctional magnetic Fe_3O_4/nitrogen-doped porous carbon NCs for the removal of organic dyes [63]. Also, g-C_3N_4 is another endogenous peroxidase-like nanozyme. In Chen's study, g-C_3N_4-Fe_3O_4 magnetic nanomaterial can be prepared by chemical coprecipitation method and used for glucose detection [64]. The Fe_3O_4/g-C_3N_4 NCs can enhance the activity of Fenton and photo-Fenton. This strengthening effect was mainly due to the effective charge transfer between Fe_3O_4 and g-C_3N_4 preventing electron hole recombination [65].

Except of inorganic nonmetallic material, same organic material also can increase the peroxidase-like activity of Fe_3O_4 nanozyme. DNA-functionalized Fe_3O_4 nanozyme with significantly enhanced peroxidase-like activity can be used to detect ions and molecules. Liu *et al.* found that DNA-modified Fe_3O_4 nanozyme had 10 times higher catalytic activity than Fe_3O_4 alone when TMB as catalytic substrate. This is because negatively charged DNA adsorbed on the surface of positively charged Fe_3O_4 nanomaterials can increases the binding capability with TMB and improves the catalytic activity [66]. Yang *et al.* reported that adenosine 5′-monophosphoric acid (AMP) can increase the peroxidase-like activity of Fe_3O_4 NPs, and verified that the Michaelis constant of Fe_3O_4 NPs with AMP was 5.3 times lower than that of bare Fe_3O_4 NPs [67]. This is because the combination of Fe^{2+}/Fe^{3+} on the surface of Fe_3O_4 NPs with AMP activates H_2O_2 to generate ·OH. Yan *et al.* simulated the catalytic microenvironment of HRP to improve the peroxidase-like activity of nanozymes [68]. The histidine was added on the surface of Fe_3O_4 nanomaterials and provided an active center similar to HRP to nanozyme. The hydrogen bond between the imidazole group of histidine and H_2O_2 increased the affinity of the nanozyme to H_2O_2. Yu *et al.* synthesized a series of nanomaterials as citrate-, glycine-, polylysine-, poly(ethyleneimine)-, carboxymethyl dextran-, and heparin modified iron oxide nanoparticles (Ncit, Ngly, NPLL, NPEI, NCMD, and Nhep), and unmodified iron oxide nanoparticles (Nnat), which have different surface charges, charge intensity and coating thickness [69]. The results show that the negatively charged nanomaterial modified with heparin has stronger affinity for TMB and the positively charged nanomaterial modified with poly(ethyleneimine) has a stronger affinity for ABTS.

Therefore, in order to improve the catalytic activity of Fe_3O_4 nanozyme, material modification is an effective method. The first way, noble metals (*e.g.*, Au, Pd, Pt) with peroxidase-like activity were coated on Fe_3O_4 nanozymes, and the synergistic effect enhanced the catalytic performance. The second way, doping or surface modification by elements, such as Cu^{2+}, Mn^{2+} on the Fe_3O_4 can help to activate and decompose H_2O_2, and improve the reaction speed. Another way is to change the surface charge of Fe_3O_4 nanozyme charge by modifying, which would enhance the electrostatic attraction, so that the nanozyme presented higher affinity and catalytic activity for the chromogenic substrate.

3. Catalytic mechanism and affect factors

3.1. Catalytic mechanism

Most of the research on mimic enzymes has focused on the catalytic property. HRP, a natural peroxidase with an iron porphyrin structure as its catalytic center, has an amino acid peptide group with affinity and complexation for the substrate as a binding site. The Fe_3O_4 nanomaterials can have peroxidase-like activity mainly because they can catalyze the decomposition of H_2O_2 with Fe^{2+}/Fe^{3+} as the catalytic center. The ·OH were produced by Fenton and/or Haber-Weiss reactions [70].

The main reactions are as follows:

$$Fe^{3+} + H_2O_2 \rightarrow FeOOH^{2+} + H^+ \quad (1)$$

$$FeOOH^{2+} \rightarrow Fe^{2+} + HO_2^{\bullet} \quad (2)$$

$$Fe^{2+} + H_2O_2 \rightarrow Fe^{3+} + OH^- + {}^{\bullet}OH \quad (3)$$

According to this catalytic property, Fe_3O_4 nanozymes can catalyze the color change of different chromogenic substrates such as ABTS, DAB, OPD and TMB. Wu *et al.* reported the relationship between the chemical properties of benzidine-based substrates and the analytical performance of the chromogenic reaction [71]. For TMB, it contains two amino groups that are easy to be oxidized. The Fe_3O_4 nanozymes firstly combine with the H_2O_2 and form the intermediate ·OH. Then, TMB loses an electron in the presence of ·OH which produced by Fenton and/or Haber-Weiss reactions and form a colored charge transfer complex. The final complex consists of the parent diamine (TMB) and the diimine (TMB^{2+}). The whole reaction process caused a color change. For ABTS, the reaction catalyzed by Fe_3O_4 nanozyme can be expressed by the following formula: H_2O_2 + ABTS $\xrightarrow{Fe_3O_4}$ $2H_2O$ + oxidized ABTS. The Fe_3O_4 nanozyme catalyzes H_2O_2 and produces ·OH to oxidize ABTS as a green ABTS radical. The mechanism is similar to that of TMB oxidation. The generated ·OH will capture H^+ from ABTS, and the ammonia salt of ABTS loses an electron and turns into green cation radical $ABTS^+$. As a colorless chemical substance, OPD can be oxidized form orange oxidation product 2,3-diaminophenazine by Fe_3O_4 nanozyme. Similarly, DAB is oxidized to brown products in the presence of Fe_3O_4 and H_2O_2. In summary, the enzymatic reaction can be summarized as follows: $DH_2 + H_2O_2 \xrightarrow{Fe_3O_4} D + 2H_2O$. DH_2 is the reducing dye hydrogen donor, and D is the generated colored oxidation-type dye.

In order to get insight into the catalytic mechanism of the Fe_3O_4 nanozymes, the steady-state kinetic parameters of the reaction were usually calculated by established Michaelis-Menten equation through using TMB or H_2O_2 as substrates. The experiments were carried out by changing the concentration of one substrate [72]. Liang *et al.* proposed a protocol that can complete the measurement of catalytic activity of the nanozyme within 4 h, which offered a standardized method for the catalytic activity comparison of various Fe_3O_4 nanozymes [73]. In this work, the unit used to compare the catalytic activity of nanozymes means the amount of nanozymes that can catalyze 1 μmol of product in one minute. The catalytic properties of standardized nanozymes depend on their kinetic constants. The kinetics of the Fe_3O_4 nanozyme follow the Michaelis-Menten equation: $\nu = (\nu_{max}[s])/(k_M+[s])$, where ν is the initial rate of reaction, ν_{max} is the maximum rate of reaction observed at the concentration of the saturated substrate, $[s]$ is the concentration of the substrate, and k_M reflects the affinity of the nanozyme for its substrate. The obtained data were fitted by the Lineweaver-Burk plot to calculate the ν_{max} and k_M value. The k_M value is recognized as an indicator of enzyme affinity to substrates. The smaller the k_M value is, the greater the affinity of the material to the substrate.

3.2. Affecting factors

Mostly of natural enzymes are proteins that can easily be deactivated by external conditions. Therefore, artificial simulated nanozymes have been hoped to be a good substitute. However, the activity of Fe_3O_4 nanozymes is affected by some factors. We discussed the effects of size, structure, reaction environment, *etc.*, on the peroxidase-like activity of Fe_3O_4 nanozymes.

3.2.1. Size

Size is one important factor affecting the peroxidase-like activity of Fe_3O_4 nanozymes. It has been reported that the peroxidase-like activity of Fe_3O_4 NPs increases with decreasing size. Smaller nanomaterials would have a larger specific surface area, and more exposed active sites. Therefore, the Fe_3O_4 NPs can more conveniently bond with the substrate for catalytic reactions. In 2007, Yan *et al.* found that Fe_3O_4 NPs had intrinsic peroxidase-like activity, and analyzed the effect of different size Fe_3O_4 NPs: 30 nm, 150 nm and 300 nm. The results showed that at 30 nm, the Fe_3O_4 NPs had the highest activity, and the activity decreased with the size increased [5]. After that, Gu *et al.* synthesized three Fe_3O_4 NPs with

different sizes: 11 nm, 20 nm and 150 nm [74], and the catalytic activity was inversely proportional to the material size.

3.2.2. Structure

Material structure is another important factor affecting the peroxidase-like activity. Different structures of materials have different crystal planes. Liu *et al.* synthesized three different structures of Fe_3O_4 nanocrystals as cluster spheres, triangular plates, and octahedral, and investigated the effect of the structure on peroxidase-like activity, respectively [75]. For these three Fe_3O_4 nanocrystals, the lattice fringe spacing were 0.253 nm, 0.299 nm, and 0.495 nm corresponding to the (311), (220) and (111) planes of the cubic magnetite phase, respectively. These crystal planes could adsorb H_2O_2 on the surface and break H_2O_2 into two ·OH radicals, and lead to the further catalytic reaction. The arrangement of atoms on each crystal surfaces would affect the electron transfer ability of the materials, which would result in different adsorption energies on H_2O_2. Therefore, the peroxidase catalytic activity of each structure has significant difference, and presented an order of cluster spheres > triangular plate > octahedron. The cluster spheres with (311) plane has the largest specific surface area and more catalytically active iron atoms on the surface, which showed the highest catalytic activity. The lowest k_M value (0.23 mmol/L) of cluster spheres means it can more efficient affinity with the substrate (H_2O_2). The octahedra with (111) plane had less open plane and dangling bonds than that of triangular plate with (220) crystal plane, which showed the worst affinity for substrates. Therefore, triangular plates with the k_M value as 0.46 mmol/L exhibited a superior catalytic activity than the octahedral with the k_M value as 0.58 mmol/L.

3.2.3. Reaction environmental conditions

The pH value is also an important factor that can affect the catalytic activity of nanozymes. When Fe_3O_4 NPs were first found to have peroxidase-like activity, the optimal pH value for the catalytic activity of Fe_3O_4 nanomaterials was 3.5, which limited the application of Fe_3O_4 nanozymes. Therefore, many researchers are devoted to solving the problem. Singh *et al.* used ATP to regulate the pH, and the peroxidase-like activity of Fe_3O_4 NPs was enhanced over a wide pH range, which could detect glucose in human serum under physiological pH [76]. Gu *et al.* verified the effect of Fe_3O_4 nanozyme on H_2O_2 under different pH conditions [77]. At pH 4.8, Fe_3O_4 nanozyme can catalyze H_2O_2 to generate ·OH and oxidize the color substrate. However, at pH 7.4, Fe_3O_4 NPs have the activity similar to catalase, which can decompose H_2O_2 into water and oxygen. The biological buffer also can affect the peroxidase-like activity of Fe_3O_4 nanozymes by interacting with the surface of the material. Enio *et al.* investigated the activity of nanozymes in acetic acid, phosphate and HEPES buffer solution [78]. Due to the interaction between anions and nanozymes, and the surface passivation of nanozymes, the biological buffer reagents with similar physiological conditions can inhibit the peroxidase-like activity of nanozymes. Therefore, the biological buffer solution is also a key influencing factor to be considered.

In conclusion, the peroxidase-like activity of Fe_3O_4 nanozymes could be affected by size, structure, reaction environment and other factors. In general, the particle with smaller size will lead to a better catalytic performance due to the larger specific surface area. Different structure of Fe_3O_4 nanozymes will causes the change of lattice fringe spacing and plane, which will affect their peroxidase-like activities due to the difference of exposed active sites. These two factors are ultimately related to the synthesis and modification method. However, the environmental condition is another important factor which can directly affect the peroxidase-like activity of nanozymes in practical application. Therefore, it is crucial to select a suitable detection condition.

4. Applications of Fe_3O_4 nanozymes

Research on the peroxidase-like activity of Fe_3O_4 nanozymes has become increasingly popular and attracted researchers' attention in practical applications. The applications of Fe_3O_4 nanozymes in analytical chemistry have been listed in Table 2.

4.1. Food safety analysis

As people taken increasing attention on food safety, the rapid, convenient and sensitive detection method based on Fe_3O_4 nanozymes has a great future in food safety analysis. The detection targets include nutrient components and exogenous contaminants.

4.1.1. Food composition analysis

AA, also known as vitamin C, can improve the body's immunity, and AA deficiency will lead to scurvy. Lu *et al.* synthesized carbon dots (CDs)/Fe_3O_4 hybrid nanofibers based on electrostatic spinning technology, hydrothermal reactions and thermochemical reduction methods for the sensitive detection of AA [79]. The synergy between CDs and Fe_3O_4 make composite materials take better peroxidase-like activity. As the presence of AA can effectively inhibit the oxidation of TMB, it can be detected with a linear range of 1–30 μmol/L and limit of detection (LOD) value at 0.285 μmol/L. Guan *et al.* loaded Au NPs onto Fe_3O_4 NPs and synthesized gold and magnetic particles for AA colorimetric detection [80]. The Au NPs not only improved the peroxidase-like activity but also improved the stability of the material. As the ABTS can be catalyzed to show green, AA could clear ABTS free radicals in the system and eliminate the color. This method can be used to detect AA in beverages with the LOD value as 0.12 μmol/L.

Glucose is an indispensable substance in life activities. Fu *et al.* synthesized Fe_3O_4@Au-PB, a type of nanomaterial with Fe_3O_4 MNPs as a magnetic core and double shells consisting of PB and Au, for glucose detection in wine samples [81]. The synergy of the multilayer shell causes the material having better activity than that of the Fe_3O_4 nanozyme alone. Jiang *et al.* prepared a sandwich structure magnetic microsphere (Fe_3O_4@RF-Pt@PDA) for glucose detection with a detection limit as 1.36 μmol/L [55]. This structure can not only provide more active sites for Pt but also improve the stability. Therefore, this multifunctional microsphere can have superior peroxidase-like activity.

4.1.2. Food contamination analysis

Food contaminants include pathogenic microorganisms, food additives, residual antibiotics, and so on. They can be enriched in the human body and cause disease or injury. Therefore, many sensitive methods have been developed for the detection of them.

Food additives are nonnutritive substances that can be used for the improvement of food appearance, flavor and texture or storage properties. L-cysteine is used to prevent vitamins being oxidized and discolored in fruit juices or fermented flour products. In Lu's work, Fe_3O_4 nanofibers with excellent peroxidase-like activity were prepared by polymer-assisted thermochemical reduction method for the sensitive detection of L-cysteine [82]. This one-dimensional (1D) morphology Fe_3O_4 nanofibers have better peroxidase-like activity than common NPs based on the large specific surface area and strong redox activity offered by the influence of morphology and structure. The L-cysteine can bind to Fe^{3+} and inhibit catalyzed oxidation to induce blue degeneration. Therefore, the detection sensitivity of L-cysteine is improved as 0.028 μmol/L. Antibiotic residues in animal-based foods can migrate into the human body and cause a series of harms. Li *et al.* developed a colorimetric biosensor to detect tetracyclines (TCs) based on the peroxidase-like activity of Fe_3O_4 MNPs [83]. TCs can combine with Fe^{2+} and Fe^{3+} on the surface of Fe_3O_4 NPs and enhance the catalytic activity by

Table 2
A list of applications of Fe_3O_4 nanozyme in analytical chemistry and its catalytic kinetic parameters.

Application		Analyte	Real sample	LOD	Linear range	Substrate	k_M (mmpl/L)	V_{max} (10^{-8} mol/s)	Ref.
Food safety analysis	Food composition analysis	AA	Drink	0.12 μmol/L	0.01–1 mmol/L	ABTS	0.265		[80]
						H_2O_2	0.51		
		Glucose	Fruit juices	1.36 μmol/L	0.01–4 mmol/L	TMB	0.187	23.84	[55]
						H_2O_2	0.289	13.56	
	Food contamination analysis	L-cysteine		0.028 μmol/L	2–10 μmol/L	TMB	0.45		[82]
						H_2O_2	18.71		
		OTA	Cereal	30 pg/mL	0.5–100 ng/mL	H_2O_2	4.27	2.89	[40]
		OP	Environmental water, apple juice	0.2 nmol/L	0.5–500 nmol/L	TMB	0.692	3.56	[87]
						H_2O_2	0.030	1.52	
		Atrazine	Water	2.89 μg/L	2–20 μg/L	TMB	0.125	5.23	[88]
						H_2O_2	0.086	9.46	
Industrial pollution analysis	Inorganic ions	PO_4^{3-}	Tap and river water	49.8 nmol/L	0.066–33.3 μmol/L	TMB	0.4	70.87	[90]
						H_2O_2	12.8	8.29	
	Chemical pollutant	PNP	Water	45 nmol/L	0.1–10 μmol/L	TMB	0.059	48.7	[91]
						H_2O_2	0.65	94.3	
		PFOS	Water	8.6 nmol/L	0.1–12.5 μmol/L	TMB	0.35	35	[93]
						H_2O_2	2.5	3.3	
Biosafety analysis and detection		H_2O_2		0.212 μmol/L	2.5–100 μmol/L	H_2O_2	0.228	3.166	[51]
						TMB	0.220	3.124	
		Cholesterol	Serum	0.8 μmol/L	2–50 μmol/L	TMB	0.112	11.42	[99]
						H_2O_2	0.077	17.95	
		PDGF-BB	Serum	50 amol/L	1–10^6 fmol/L	TMB	0.2	1.34	[102]
						H_2O_2	0.23	2.41	
		DNA/microRNA	Serum	0.15 amol/L	0.5–10^6 amol/L	TMB	0.022		[103]
						H_2O_2	0.19		
		ATP	Blood	0.09 μmol/L	0.50–100 μmol/L	TMB	0.088	0.406	[105]
						H_2O_2	30.24	0.342	

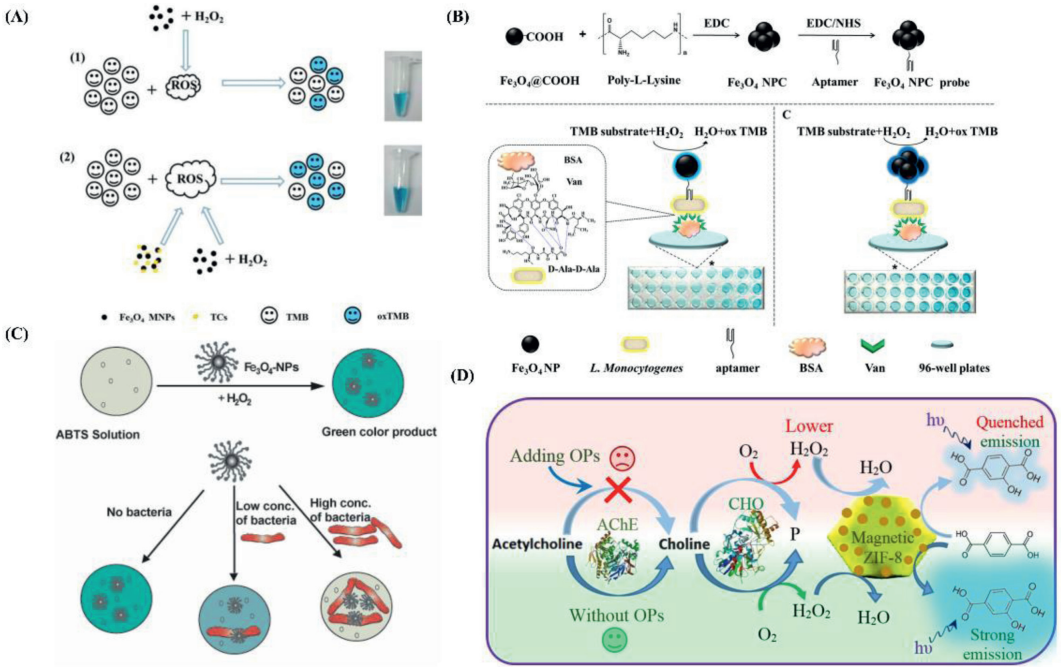

Fig. 2. The mechanism of iron-based nanomaterials analysis and detection for food contaminants. (A) A noble colorimetric biosensor for the determination of tetracyclines. Copied with permission [83]. Copyright 2016, Elsevier. (B) The biosensor for the determination of *L. monocytogenes*. Copied with permission [84]. Copyright 2016, Elsevier. (C) Catalytically amplified colorimetric sensing of bacteria by using Dop-Fe_3O_4 NPs as enzymatic mimetic. Copied with permission [85]. Copyright 2017, Royal Society of Chemistry. (D) The schematic illustration of detection of OPs. Copied with permission [87]. Copyright 2019, Elsevier.

the multitudinous O- and N-groups. Therefore, the tracycline, TC and doxycycline can be detected by this biosensor with detection limits of 26 nmol/L, 45 nmol/L and 48 nmol/L, respectively (Fig. 2A).

Bacterial infect is another common food contamination type. Common foodborne bacteria include *Escherichia coli* O157:H7 (*E. coli*), *Staphylococcus aureus*, *Salmonella enterica*, *Listeria monocytogenes* (*L. monocytogenes*) and so on. Xing and Zhou *et al.* prepared a biosensor for *L. monocytogenes* detection with Fe_3O_4 nanoparticle cluster (NPC) modified with aptamer as specific recognizer and vancomycin (Van) as molecular recognition agent [84]. The aptamer and Van can specifically bind to *L. monocytogenes*, and form a special structure for colorimetric detection. With higher catalytic activity, the Fe_3O_4 NPC improved detection sensitivity as the visual detection limit at 5.4×10^3 cfu/mL (Fig. 2B). Also, using Fe_3O_4 nanomaterials for simple and rapid detection of *E. coli* has been reported successively. Hussain *et al.* reported a dopamine-modified Fe_3O_4 NPs (Dop-Fe_3O_4 NPs) that have been used for signal amplification to detect *E. coli* [85]. This Fe_3O_4 nanozyme can oxidize ABTS into green products in the presence of H_2O_2. However, the anions on the bacterial surface can combine with the cations on the NPs due to electrostatic action, inhibit the peroxidase-like activity and prevent the colorimetric reaction (Fig. 2C). Therefore, the visually LOD value of *E. coli* is 10^4 cfu/mL, and the LOD value of *E. coli* can be improved to 10^2 cfu/mL by spectrophotometry.

Mycotoxins are also a major source of food problems. Ochratoxin A (OTA) is one of the most common natural mycotoxins that can cause kidney damage and harm human health. Huang *et al.* synthesized Au@Fe_3O_4 NPs for colorimetric detection of OTA with a detection limit of 30 pg/mL [39]. The DNA modified on Au@Fe_3O_4 NPs can be hybridized with the aptamer to capture the target. When OTA exists, it is firstly ~~be~~ recognized by the aptamer and releases Au@Fe_3O_4 NPs, which can oxidize TMB to blue in the presence of H_2O_2.

With excessive use and migration, pesticides become serious environmental pollution [86]. Khataee and Habibi *et al.* developed a fluorescence analysis method for the detection of organophosphorus (OP) [87]. Fe_3O_4 was encapsulated in zeolitic imidazolate frameworks (ZIFs). For OP detection, H_2O_2 is produced by AChE and ChOx firstly, and then a chromogenic reaction occurs under the effect of the Fe_3O_4 NPs@ZIF-8 with TMB (Fig. 2D). The OP can inhibit the activity of AChE and stop the reaction. Atrazine, a type of herbicide, has poor biodegradability and can cause various adverse reactions. For the detection and degradation of Atrazine, Fe_3O_4 NPs and TiO_2 NPs were fixed on graphene to obtain Fe_3O_4-TiO_2/rGO composite [88]. Atrazine can react with TMB and form hydrogen bonds to inhibit TMB oxidation. Therefore, the concentration of atrazine is inversely proportional to the gradation of color. The LOD value is 2.89 μg/L, and the linear range is 2–20 μg/L.

4.2. Industrial pollution analysis

With the rapid development of industrialization, pollution is worsening and endangering human health.

As a type of heavy metal ion, Hg^{2+} is highly toxic and becomes more virulent after being converted to organic mercury. Therefore, sensitive detection of Hg^{2+} has great significance for environmental monitoring. Cysteine (Cys) can reduce the free radical cation produced in the chromogenic reaction and block the chromogenic reaction progress. However, Hg^{2+} can interact with the sulfhydryl group of Cys and make the blocked progress recover. Niu *et al.* synthesized Cys-modified Fe_3O_4 MNPs for the detection of Hg^{2+} [89]. First, Cys was coated on Fe_3O_4 and blocked the active site. When Hg^{2+} is present, Cys spalls and exposes the active site of Fe_3O_4 based on the coordination function of Cys-Hg^{2+}-Cys. Then, the peroxidase-like activity of Fe_3O_4 recover (Fig. 3A). This method can be used for ultrasensitive detection of Hg^{2+} with LOD value as 5.9 pmol/L in real samples as river water, human serum and urine. Phosphate (PO_4^{3-}) also widely exists in the environment, and will cause environmental pollution and harm human health. Ni *et al.* modified 3,4-dihydroxycinnamic acid (DHCA) on Fe_3O_4 and produced Fe_3O_4-DHCA nanocubes for selective detection of PO_4^{3-} [90]. Hydrophilic DHCA improves the catalytic activity and disper-

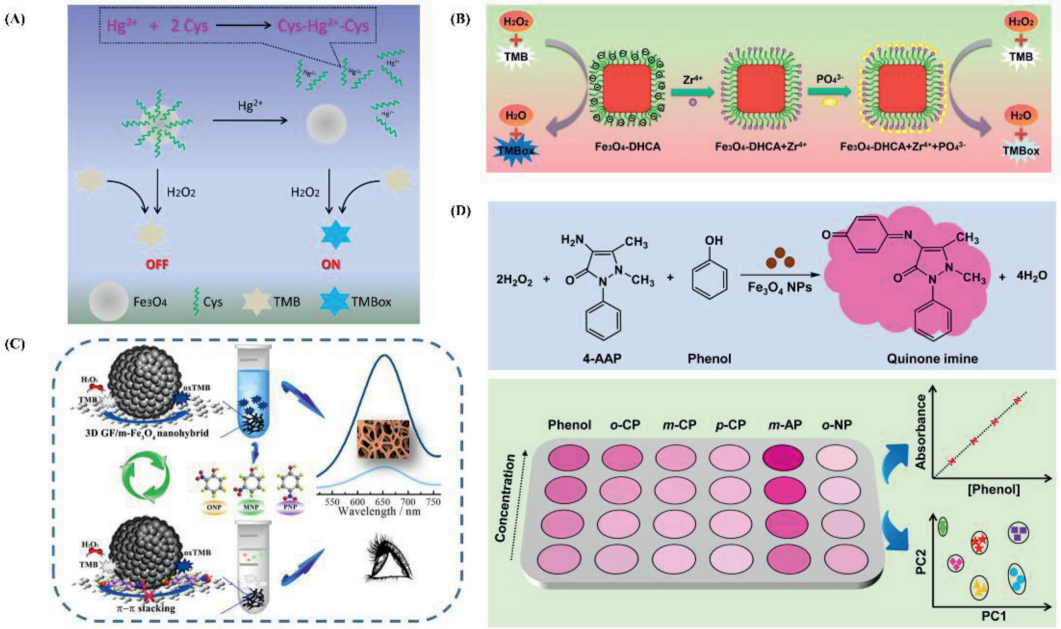

Fig. 3. The mechanism of Fe_3O_4 nanozyme analysis and detection of industrial pollutants. (A) Principle for the sensing of Hg^{2+}. Copied with permission [89]. Copyright 2019, Elsevier. (B) Schematic illustration of the detection of PO_4^{3-}. Copied with permission [90]. Copyright 2019, Elsevier. (C) Schematic representation of selective colorimetric determination of PNP. Copied with permission [91]. Copyright 2018, Elsevier. (D) Colorimetric quantification and discrimination of phenolic pollutants. Copied with permission [92]. Copyright 2020, Elsevier.

sion performance of the material. When PO_4^{3-} exists, a film will be formed on the surface of the material due to the specific interaction between Zr^{4+} and PO_4^{3-}, and inhibit peroxidase-like activity and stop the chromogenic reaction (Fig. 3B).

Phenolic compounds are a large class of hazardous chemical pollutants that have serious toxicity. *p*-Nitrophenol (PNP) is a phenolic compound with highly toxic and difficult to degrade. The United States Environmental Protection Agency listed it in the "list of priority pollutants". Guo *et al.* used 3D graphene as the carrier and synthesized 3D graphene/mesoporous Fe_3O_4 (3D GF/m-Fe_3O_4) nanozymes as colorimetric sensors for PNP detection [91]. The synergistic effect between 3D GF and m-Fe_3O_4 can enhance the peroxidase-like activity. However, PNP can adsorb on the active site of nanozymes by π-π interactions and inhibits peroxidase-like activity. Therefore, the sensor has good selectivity to PNP in the presence of three NP isomers, with the detection limit at 45 nmol/L (Fig. 3C). Recently, Niu and Pan *et al.* used the peroxidase-like activity of Fe_3O_4 nanozymes to catalyze the colorless 4-aminoantipyrine to turn pink in the presence of phenol. And this method has excellent specificity for phenol rather than six other common phenolic pollutants (Fig. 3D) [92].

Perfluorooctane sulfonate (PFOS) is widely used in textile processing with the characteristics of bioaccumulation and difficult to degrade. Zhao *et al.* used solvent heat method to anchor Fe_3O_4 NPs on MoS_2 with petal shapes and synthesized a MoS_2/Fe_3O_4 NC [93]. The synergistic reaction between MoS_2 and Fe_3O_4 NPs enhances the catalytic activity of this material. The PFOS can adsorb on the Fe_3O_4 NPs by electrostatic action and cover the reactive center to inhibit the catalytic reaction result in lighter blue reaction solution. Phenylenediamine is an important dye intermediate but can cause serious environmental pollution. In order to identify isomers as OPD, *m*-phenylenediamine (MPD) and *p*-phenylenediamine (PPD), Zhao *et al.* synthesized Fe_3O_4 NP/nitrogen-doped graphene quantum dots (Fe_3O_4/N-GQDs) with large specific surface area as carriers for the visual identification [94]. N-GQDs are used for Fe^{3+} reduction and material stability improvement. The ·OH will be produced with the presence of H_2O_2, and then different colors will be observed with the oxidization of different isomers. In this work, the detection limits of OPD and PPD were 0.23 μmol/L and 0.53 μmol/L, respectively.

4.3. Biosafety analysis and detection

In recent years, Fe_3O_4 nanozymes with peroxidase-like activity have also been applied in biosafety detection.

H_2O_2 is special marker of reactive oxygen, and the accumulation of H_2O_2 in cells will produces toxic effects and leads to some diseases. Hou *et al.* used the three-dimensional graphene (3DG) network as a carrier to load Fe_3O_4 QDs and synthesized Fe_3O_4/3DG-NCs for the detection of H_2O_2 released by A549 human lung cancer cells [95]. The 3DG network with high specific surface area can not only increase the active center of Fe_3O_4 for H_2O_2 reduction but also improve the stability of Fe_3O_4 and prevent agglomeration. Sun *et al.* loaded Fe_3O_4@ZIF-8 on molybdenum disulfide (MoS_2) nanosheets and deposited gold nanoflowers (Au NFs) to obtain Au NFs/Fe_3O_4@ZIF-8-MoS_2 for the detection of H_2O_2 released by H9C2 cardiac cells [24]. In addition, nanozymes with peroxidase-like activity are also very popular in tumor treatment. The nanozymes can catalyze H_2O_2 to produce ·OH to kills cancer cells (Fig. 4A). Lin *et al.* combined Fe_3O_4 nanomaterials with Bi_2S_3 semiconductors [96]. With the excellent performance of Bi_2S_3 in the near infrared region, this composite material has an excellent photothermal effect and can improve the peroxidase-like activity, promoting the generation of reactive oxygen species. Therefore, it can not only kill cancer cells without destroying cells but also has infrared thermal imaging and photoacoustic imaging capabilities. In addition, nanozymes with peroxidase-like activity can destroy cell membranes by producing ·OH to achieve antibacterial effects [97].

For blood sugar detection, MNPs-glucose oxidase (GOx)-nanoflowers based on the action of copper sulfate crystallization were synthesized [98]. Glucose first generates H_2O_2 under the ac-

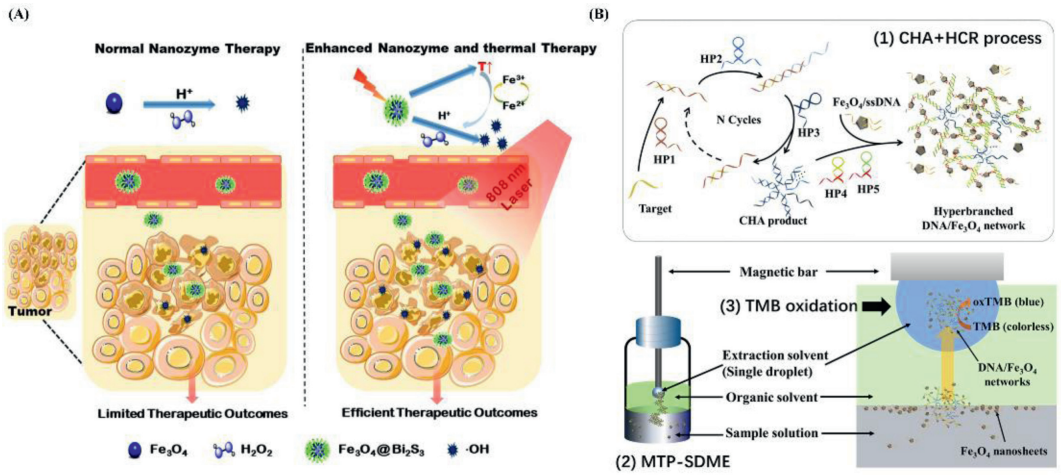

Fig. 4. The mechanism of Fe_3O_4 nanozyme for biosafety analysis and detection. (A) Schematic diagram for *in vivo* photothermal and photothermal-enhanced nanozymatic catalytic tumor-specifc sequential therapeutic mechanism under 808 nm. Copied with permission [96]. Copyright 2020, Elsevier. (B) The schematic illustration of magnetic three-phase single-drop microextraction for DNA and microRNA analysis. Copied with permission [14]. Copyright 2020, American Chemical Society.

tion of GOx in the nanoflowers, and then the nanomaterial with peroxidase-like activity converts the Amplex UltraRed substrate into a highly fluorescent product in the presence of H_2O_2.

Cholesterol can be oxidized by cholesterol oxidase and generate H_2O_2 in the presence of O_2. Therefore, cholesterol can be detected by H_2O_2 content determination. Hu *et al.* synthesized Fe_3O_4@MIL-100 (Fe) [99]. Fe_3O_4 can work synergistically with MIL-100 (Fe), which has endogenous peroxidase-like activity, to improve the catalytic activity. Ye *et al.* doped Cu in Fe_3O_4@FeOOH to synthesize Cu/Fe_3O_4@FeOOH NCs for cholesterol detection [100]. After doping with Cu, the formed oxygen vacancy can promote the decomposition of H_2O_2, which can enhance the oxidation of the composite material to TMB. Therefore, the synergistic effect between Cu, Fe_3O_4 and FeOOH can significantly enhance the peroxidase-like activity performance.

Mucin-1 (MUC1) is an important tumor biomarker. Chai and Yuan *et al.* proposed an ultrasensitive method for MUC1 detection by electrochemiluminescence (ECL) immunosensor with LOD value at 4.5 fg/mL [101]. They synthesized luminol capped Au NPs (Lu–Au NPs)@Fe_3O_4 NCs as a signal marker and Au NPs@ZnO as ECL immunosensing interface. Both of these materials were connected by MUC1 antibody. In Lu–Au NPs@Fe_3O_4, Fe_3O_4 can decompose H_2O_2 to produce O_2 and oxidize luminol. In Au NPs@ZnO, ZnO plays the same role as Fe_3O_4 and improves the luminescence efficiency, too. Platelet-derived growth factor BB (PDGF-BB) has the ability to promote wound healing. Zhang *et al.* proposed the naked eye colorimetric detection method with the nanozyme-linked aptamer sorbent assay method, and the detection limit was 10 fmol/L [102]. The synthesized 1D-Fe_3O_4@C core-shell nanowires (NWS) with peroxidase-like activity can catalyze TMB. The aptamer for PDGF-BB connected to Fe_3O_4@C NWS and the microplate surface is used as reporter probe and capture probe, respectively. When PDGF-BB exists, the aptamer specifically binds to it, and then Fe_3O_4@C NWs catalyze TMB and cause the chromogenic reaction.

The normal expression of microRNAs is closely related to human health [15]. Tang and Shen *et al.* detected the microRNA let-7a with high sensitivity by synergistic effects of three amplification methods: hybrid chain reaction (HCR), network structure and Fe_3O_4 peroxidase-like activity [103]. DNA strands were fixed onto the surface of Fe_3O_4 nanosheets to form a two-dimensional network structure through HCR reaction, and then catalyzed the TMB reaction through the peroxidase-like activity of Fe_3O_4. The detection limit for let-7a is 13 amol/L. Subsequently, Tang *et al.* used a catalytic hairpin assembly and HCR to form a DNA/Fe_3O_4 network through a target-triggered cyclic amplification strategy and combined it with magnetic three-phase single drop microextraction (MTP-SDME) to detect DNA and microRNA [14]. The formed

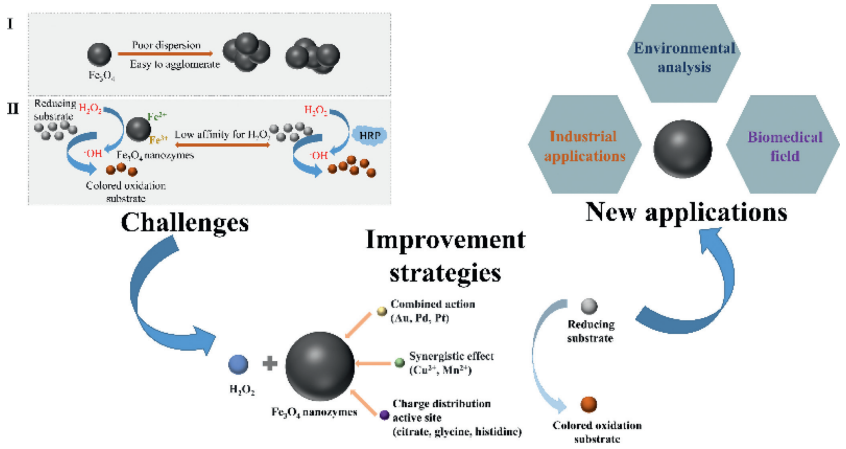

Fig. 5. The current challenges and future outlook.

network structure can be quickly separated by MTP-SDME and then further catalyze the oxidation of TMB in tiny droplets, which greatly improves the detection result (Fig. 4B). Tian *et al.* fixed a hairpin capture probe onto the surface of Fe_3O_4 NPs and combined it with microRNA-21 to perform an HCR reaction. The planar Cu complex was combined with the DNA structure through hydrogen bonding, and improved the peroxidase-like activity by the synergistic effect between Fe_3O_4. The detection limit for microRNA-21 is 33 amol/L, and the detection result ranges from 100 amol/L to 100 nmol/L [104].

Wang *et al.* reported a method for trace ATP detection in blood with Fe_3O_4 nanozyme with detection limit of 0.09 μmol/L [105]. ATP-specific aptamers (Apts) are immobilized on the surface of Fe_3O_4 NPs, and the bases can react with TMB through hydrogen bonding and π-π stacking, which can increase its catalytic activity by 6 times. When ATP is present, Apts first reacts with ATP, which causes Apts to precipitate out of the Fe_3O_4 NPs, thereby reducing the catalytic activity and correspondingly lightening the color.

5. Conclusions and outlook

The discovery of peroxidase-like activities similar to those of HRP of Fe_3O_4 nanomaterials has laid the foundation for the colorimetric detection. In this article, we have listed several methods for the synthesis of Fe_3O_4 nanozyme and introduced the effects of different synthesis methods on product characteristics in shapes and sizes. The modification methods with different materials and methods to improve the peroxidase-like activity of nanozyme is another important part in this article. Therefore, a suitable method can be chosen based on the actual needs according to these studies. Also, the catalytic activity and kinetic mechanism of Fe_3O_4 nanomaterials were summarized in this article to parse the catalytic mechanism of nanozymes. The influence of different factors as particle size, structure, environment on the peroxidase-like activity of Fe_3O_4 nanozymes has been thoroughly analyzed (Fig. 5).

To date, Fe_3O_4 nanozymes have been found to have peroxidase-like activity for more than ten years. With both excellent magnetic properties and peroxidase-like properties, Fe_3O_4 nanozymes were widely used in food analysis, industrial pollutant detection, biological analysis, and other fields and continues to deepen research. In the food safety analysis, we mainly summarized the analysis and detection of food components and exogenous contaminants. In the industrial pollutant detection, we mainly summarized the colorimetric detection of inorganic ions, pesticides, dyes and phenolic pollutants. In the field of biosafety diagnosis, it mainly focuses on the rigorous analysis and detection of substances in cells and blood.

As artificial peroxidase-like mimics, Fe_3O_4 nanozymes have replaced natural enzymes, which are easily inactivated due to external environmental influences and expensive, and have the advantages of good stability, low cost and easy production. However, there are still some challenges that need to be overcome. (1) The catalytic activity of Fe_3O_4 nanozymes can be further enhanced. According to the kinetic parameters, the Fe_3O_4 nanozyme has a higher affinity than HRP with substrate TMB. So, the situation is the opposite when the substrate is H_2O_2. Therefore, the low affinity for H_2O_2 is an important restriction for the enhancement of enzyme activity. Fortunately, the catalytic activity of artificial nanozymes can be altered by a series of surface modifications or additives. Therefore, how to obtain higher peroxidase-like activity of Fe_3O_4 nanozymes still needs to be continuously studied. Nevertheless, the design of novel modification methods and the development of synergistic materials will be important ways to improve the catalytic activity of Fe_3O_4 nanozymes. (2) Catalytic mechanism of Fe_3O_4 nanozymes and the modified composites need to be studied deeply. Some mechanism has been summarized in this article. For example, some noble metal materials have the similar catalytic mechanism to Fe_3O_4 and can improve the catalytic activity of Fe_3O_4 by modification. The peroxidase-like activity of them is implemented by surface adsorption of H_2O_2 and fast electron transfer with H_2O_2 to produce ·OH; some other metal materials can act synergistically with Fe_3O_4 and enhanced the decomposition of H_2O_2 to improve the peroxidase-like activity of composite materials. Cu^{2+} has the similar ion radii of Fe^{2+} and can replace Fe^{2+} in a certain extent and reduce Fe^{3+} to Fe^{2+}. Also, the Cu^{2+} ions can be enriched on the surface of composite materials and promote the regeneration of Fe^{2+}; most of the nonmetal materials can improve the catalytic activity of composite materials by increasing the affinity capability of Fe_3O_4 to substrate through changing the surface charge distribution or providing active centers to substrate. However, more questions still need to be addressed. For example, the effect of different components or the structure of Fe_3O_4 nanozymes on the catalytic performance is unclear in most cases. Through studying of electrostatic adsorption, electron transfer and valence state of Fe_3O_4 nanozymes composite, we can further explore the catalytic mechanism. The study of catalytic mechanism can provide theoretical basis for the design of novel modification methods and the development of synergistic materials. (3) Currently, the application of Fe_3O_4 nanozyme is mainly in the fields of food, environment, and biosafety. Compared with other methods, the Fe_3O_4 nanozyme-based detection process is lower in cost and shorter time-consuming. It also presents great potential of broad prospects in many other fields in future study.

Declaration of competing interest

The authors declare that they have no known competing financial interests or personal relationships that could have appeared to influence the work reported in this paper.

Acknowledgments

The authors are grateful for the financial support from the National Natural Science Foundation of China (Nos. 31901799, 21705060, 21605105 and 32001804), the Natural Science Foundation of Jiangsu Province, China (Nos. BK20211340 and BK20180979), Opening Project of Key Laboratory of Impurity Spectrum of Chemical Drug, China (No. NMPA-KLIPCD-2020-09) and the Emerging science and technology innovation team funding of JUST (No. 1182921902).

References

[1] C. Yuan, X. Wang, X. Yang, et al., Chin. Chem. Lett. 32 (2021) 2079–2085.
[2] X. Chen, J. Mao, C. Liu, et al., Chin. Chem. Lett. 31 (2020) 3205–3208.
[3] Z. Zhou, L. Yang, J. Gao, X. Chen, Adv. Mater. 31 (2019) e1804567.
[4] Z. Qi, T.P. Joshi, R. Liu, H. Liu, J. Qu, J. Hazard. Mater. 329 (2017) 193–204.
[5] L. Gao, J. Zhuang, L. Nie, et al., Nat. Nanotechnol. 2 (2007) 577–583.
[6] X. Liu, D. Huang, C. Lai, et al., Small 15 (2019) e1900133.
[7] Z. Li, Y. Wang, Y. Ni, S. Kokot, Biosens. Bioelectron. 70 (2015) 246–253.
[8] Y. Yang, T. Li, Y. Qin, L. Zhang, Y. Chen, Front. Chem. 8 (2020) e564968.
[9] H. Sun, Y. Zhou, J. Ren, X. Qu, Angew. Chem. Int. Ed. 57 (2018) 9224–9237.
[10] G. Nie, L. Zhang, J. Lei, et al., J. Mater. Chem. A 2 (2014) 2910–2914.
[11] L. Chen, L. Sha, Y. Qiu, et al., Nanoscale 7 (2015) 3300–3308.
[12] W. Zhang, X. Niu, S. Meng, et al., Sens. Actuators B: Chem. 273 (2018) 400–407.
[13] A. Liu, M. Li, J. Wang, et al., Chin. Chem. Lett. 31 (2020) 1133–1136.
[14] S. Tang, T. Qi, Y. Yao, et al., Anal. Chem. 92 (2020) 12290–12296.
[15] S. Tang, Y. Li, A. Zhu, et al., Chem. Commun. 55 (2019) 8386–8389.
[16] H. Wei, E.J.A.C. Wang, Anal. Chem. 80 (2008) 2250–2254.
[17] Y. Zhuo, P.X. Yuan, R. Yuan, Y.Q. Chai, C.L. Hong, Biomaterials 30 (2009) 2284–2290.
[18] G. Guan, L. Yang, Q. Mei, et al., Anal. Chem. 84 (2012) 9492–9497.
[19] M. Liang, K. Fan, Y. Pan, et al., Anal. Chem. 85 (2013) 308–312.
[20] Y. Yao, J. Kuang, J. Ju, et al., Sens. Actuators B: Chem. 352 (2022) 131044.
[21] D. Duan, K. Fan, D. Zhang, et al., Biosens. Bioelectron. 74 (2015) 134–141.
[22] N. Yu, T. Cai, Y. Sun, et al., Int. J. Pharm. 552 (2018) 277–287.
[23] F. Wei, X. Cui, Z. Wang, et al., Chem. Eng. J. 408 (2021) 127240.

[24] S. Gao, H. Lin, H. Zhang, et al., Adv. Sci. 6 (2019) 1801733.
[25] J. Lu, Y. Hu, P. Wang, et al., Sens. Actuators B: Chem. 311 (2020) 127909.
[26] F. Wu, Y. Du, J. Yang, et al., ACS Nano 16 (2022) 3647–3663.
[27] L. Huang, D.W. Sun, H. Pu, Q. Wei, Compr. Rev. Food. Sci. Food Saf. 18 (2019) 1496–1513.
[28] S. Munir, A.A. Shah, H. Rahman, et al., Biotechnol. Lett. 42 (2020) 357–373.
[29] J. Wu, X. Wang, Q. Wang, et al., Chem. Soc. Rev. 48 (2019) 1004–1076.
[30] W. Song, B. Zhao, C. Wang, Y. Ozaki, X. Lu, J. Mater. Chem. B 7 (2019) 850–875.
[31] I. Khan, A. Khalil, F. Khanday, et al., Arab. J. Sci. Eng. 43 (2018) 43–61.
[32] N. Ding, N. Yan, C. Ren, X. Chen, Anal. Chem. 82 (2010) 5897–5899.
[33] M. Zhang, T. Bu, Y. Tian, et al., Food Chem. 332 (2020) 127398.
[34] X. Li, L. Wang, D. Du, et al., TrAC Trends Anal. Chem. 120 (2019) e115653.
[35] W. Du, T. Liu, F. Xue, et al., ACS Appl. Mater. Interfaces 12 (2020) 19285–19294.
[36] L. Gao, K. Fan, X. Yan, Theranostics 7 (2017) 3207–3227.
[37] S. Zhao, X. Yu, Y. Qian, W. Chen, J. Shen, Theranostics 10 (2020) 6278–6309.
[38] S. Rajput, C.U. Pittman Jr., D. Mohan, J. Colloid Interface Sci. 468 (2016) 334–346.
[39] S. Liu, J. Fu, M. Wang, et al., J. Colloid Interface Sci. 469 (2016) 69–77.
[40] Y. Shi, J. Huang, J. Wang, P. Su, Y. Yang, Talanta 143 (2015) 457–463.
[41] Y. Shi, P. Su, Y. Wang, Y. Yang, Talanta 130 (2014) 259–264.
[42] L. Gao, K.M. Giglio, J.L. Nelson, H. Sondermann, A.J. Travis, Nanoscale 6 (2014) 2588–2593.
[43] W. Glasgow, B. Fellows, B. Qi, et al., Particuology 26 (2016) 47–53.
[44] H. Deng, X. Li, Q. Peng, et al., Angew. Chem. 117 (2005) 2842–2845.
[45] J.A. Guivar, E.G. Fernandes, V. Zucolotto, Talanta 141 (2015) 307–314.
[46] H. Wang, S. Li, Y. Si, et al., J. Mater. Chem. B 2 (2014) 4442–4448.
[47] S. Song, Y. Liu, A. Song, et al., J. Colloid Interface Sci. 506 (2017) 46–57.
[48] X. Jing, T. Liu, D. Wang, J. Liu, L. Meng, CrystEngComm 19 (2017) 5089–5099.
[49] Y. Liu, G. Zhu, C. Bao, A. Yuan, X. Shen, Chin. J. Chem. 32 (2014) 151–156.
[50] X. Huang, C. Xu, J. Ma, F. Chen, Adv. Powder Technol. 29 (2018) 796–803.
[51] H. Liu, L. Zhu, H. Ma, et al., Microchim. Acta 186 (2019) 518.
[52] C. Zheng, W. Ke, T. Yin, X. An, RSC Adv. 6 (2016) 35280–35286.
[53] W. Shi, H. Fan, S. Ai, L. Zhu, Sens. Actuators B: Chem. 221 (2015) 1515–1522.
[54] X. Xia, J. Zhang, N. Lu, et al., ACS Nano 9 (2015) 9994–10004.
[55] L. Bai, W. Jiang, M. Sang, et al., J. Mater. Chem. B 7 (2019) 4568–4580.
[56] S. Li, H. Li, F. Chen, et al., Dyes Pigm. 125 (2016) 64–71.
[57] J. Zhang, J. Ma, X. Fan, et al., Catal. Commun. 89 (2017) 148–151.
[58] F. Huang, J. Wang, W. Chen, et al., Taiwan Inst. Chem. Eng. 83 (2018) 40–49.
[59] J. Wang, F. Huang, X. Wang, et al., Process Biochem. 83 (2019) 35–43.
[60] M. Zhu, G. Diao, Nanoscale 3 (2011) 2748–2767.
[61] V. Georgakilas, J.A. Perman, J. Tucek, R. Zboril, Chem. Rev. 115 (2015) 4744–4822.
[62] N. Lu, M. Zhang, L. Ding, et al., Nanoscale 9 (2017) 4508–4515.
[63] A. Nsabimana, S.A. Kitte, F. Wu, et al., Appl. Surf. Sci. 467-468 (2019) 89–97.
[64] J. Chen, Q. Chen, J. Chen, H. Qiu, Microchim. Acta 183 (2016) 3191–3199.
[65] S. Sahar, A. Zeb, Y. Liu, N. Ullah, A. Xu, Chin. J. Catal. 38 (2017) 2110–2119.
[66] B. Liu, J. Liu, Nanoscale 7 (2015) 13831–13835.
[67] Y.C. Yang, Y.T. Wang, W.L. Tseng, ACS Appl. Mater. Interfaces 9 (2017) 10069–10077.
[68] W. Yang, J. Li, M. Wang, et al., Colloids Surf. B: Biointerfaces 188 (2020) 110742.
[69] F. Yu, Y. Huang, A.J. Cole, V.C. Yang, Biomaterials 30 (2009) 4716–4722.
[70] K. Fan, H. Wang, J. Xi, et al., Chem. Commun. 53 (2016) 424–427.
[71] X. Zhang, Q. Yang, Y. Lang, X. Jiang, P. Wu, Anal. Chem. 92 (2020) 12400–12406.
[72] W. Duan, Z. Qiu, S. Cao, et al., Biosens. Bioelectron. 196 (2022) 113724.
[73] B. Jiang, D. Duan, L. Gao, et al., Nat. Protoc. 13 (2018) 1506–1520.
[74] F.F. Peng, Y. Zhang, N. Gu, Chin. Chem. Lett. 19 (2008) 730–733.
[75] S. Liu, F. Lu, R. Xing, J.J. Zhu, Chem. Eur. J. 17 (2011) 620–625.
[76] N.V.S. Vallabani, A.S. Karakoti, S. Singh, Colloids Surf. B: Biointerfaces 153 (2017) 52–60.
[77] Z. Chen, J.J. Yin, Y.T. Zhou, et al., ACS Nano 6 (2012) 4001–4012.
[78] M. Raineri, E.L. Winkler, T.E. Torres, et al., Nanoscale 11 (2019) 18393–18406.
[79] S. Chen, M. Chi, Z. Yang, et al., Inorg. Chem. Front. 4 (2017) 1621–1627.
[80] H. Guan, B. Han, D. Gong, et al., Spectrochim. Acta A 222 (2019) 117277.
[81] Y. Li, J. Liu, Y. Fu, Q. Xie, Y. Li, Microchim. Acta 186 (2018) 20.
[82] S. Chen, M. Chi, Y. Zhu, et al., Appl. Surf. Sci. 440 (2018) 237–244.
[83] Y. Wang, Y. Sun, H. Dai, et al., Sens. Actuators B: Chem. 236 (2016) 621–626.
[84] L. Zhang, R. Huang, W. Liu, et al., Biosens. Bioelectron. 86 (2016) 1–7.
[85] S. Mumtaz, L.S. Wang, S.Z. Hussain, et al., Chem. Commun. 53 (2017) 12306–12308.
[86] Z. Wei, H. Li, J. Wu, C. Ren, et al., Chin. Chem. Lett. 31 (2020) 177–180.
[87] N. Bagheri, A. Khataee, J. Hassanzadeh, B. Habibi, Spectrochim. Acta A 209 (2019) 118–125.
[88] P.K. Boruah, M.R. Das, J. Hazard. Mater. 385 (2020) 121516.
[89] X. Niu, Y. He, X. Li, et al., Sens. Actuators B: Chem. 281 (2019) 445–452.
[90] X. Li, B. Liu, K. Ye, et al., Sens. Actuators B: Chem. 297 (2019) 126822.
[91] N. Qiu, Y. Liu, M. Xiang, et al., Sens. Actuators B: Chem. 266 (2018) 86–94.
[92] S. Wu, D. Guo, X. Xu, J. Pan, X. Niu, Sens. Actuators B: Chem. 303 (2020) 127225.
[93] J. Liu, J. Du, Y. Su, H. Zhao, Microchem. J. 149 (2019) 104019.
[94] B. Shi, Y. Su, L. Zhang, et al., Nanoscale 8 (2016) 10814–10822.
[95] Y. Zhao, D. Huo, J. Bao, et al., Sens. Actuators B: Chem. 244 (2017) 1037–1044.
[96] Y. Zhao, B. Ding, X. Xiao, et al., ACS Appl. Mater. Interfaces 12 (2020) 11320–11328.
[97] H. Wang, K. Wan, X. Shi, Adv. Mater. 31 (2019) 1805368.
[98] H.J. Cheon, M.D. Adhikari, M. Chung, et al., Adv. Healthc. Mater. 8 (2019) e1801507.
[99] Y. Wu, Y. Ma, G. Xu, et al., Sens. Actuators B: Chem. 249 (2017) 195–202.
[100] Y. Huang, G. Liang, T. Lin, et al., Anal. Bioanal. Chem. 411 (2019) 3801–3810.
[101] J.X. Wang, Y. Zhuo, Y. Zhou, R. Yuan, Y.Q. Chai, Biosens. Bioelectron. 71 (2015) 407–413.
[102] R. Zhang, N. Lu, J. Zhang, et al., Biosens. Bioelectron. 150 (2020) 111881.
[103] X. Tan, L. Zhang, Q. Tang, G. Zheng, H. Li, Microchim. Acta 186 (2019) 280.
[104] L. Tian, J. Qi, O. Oderinde, et al., Biosens. Bioelectron. 110 (2018) 110–117.
[105] S. Li, X. Zhao, X. Yu, et al., Anal. Chem. 91 (2019) 14737–14742.